Journal of Chromatography A, xxx (2019) xxx–xxx

Contents lists available at ScienceDirect

Journal of Chromatography A

journal homepage: www.elsevier.com/locate/chroma

# High throughput process development workflow with advanced decision-support for antibody purification

Christos Stamatis[a,b], Stephen Goldrick[a,b], David Gruber[b,1], Richard Turner[b], Nigel J. Titchener-Hooker[a], Suzanne S. Farid[a,*]

[a] The Advanced Centre for Biochemical Engineering, Department of Biochemical Engineering, University College London, Gower Street, London WC1E 6BT, UK
[b] MedImmune Limited, Milstein Building, Granta Park, Cambridge CB1 6GH, UK

ARTICLE INFO

*Article history:*
Received 21 November 2018
Received in revised form 28 February 2019
Accepted 3 March 2019
Available online xxx

*Keywords:*
Chromatographic antibody purification
High-throughput process development
Design of experiments
Decision-support tools
Monte Carlo simulations

ABSTRACT

Chromatography remains the workhorse in antibody purification; however process development and characterisation still require significant resources. The high number of operating parameters involved requires extensive experimentation, traditionally performed at small- and pilot-scale, leading to demands in terms of materials and time that can be a challenge. The main objective of this research was the establishment of a novel High Throughput Process Development (HTPD) workflow combining scale-down chromatography experimentation with advanced decision-support techniques in order to minimise the consumption of resources and accelerate the development timeframe. Additionally, the HTPD workflow provides a framework to rapidly manipulate large datasets in an automated fashion. The central component of the HTPD workflow is the systematic integration of a microscale chromatography experimentation strategy with an advanced chromatogram evaluation method, design of experiments (DoE) and multivariate data analysis. The outputs of this are leveraged into the screening and optimisation components of the workflow. For the screening component, a decision-support tool was developed combining different multi-criteria decision-making techniques to enable a fair comparison of a number of CEX resin candidates and determine those that demonstrate superior purification performance. This provided a rational methodology for screening chromatography resins and process parameters. For the optimisation component, the workflow leverages insights provided through screening experimentation to guide subsequent DoE experiments so as to tune significant process parameters for the selected resin. The resulting empirical correlations are linked to a stochastic modelling technique so as to predict the optimal and most robust chromatographic process parameters to achieve the desired performance criteria.



## 1. Introduction

The development of a chromatographic purification process in biopharmaceutical manufacturing is highly challenging and complex especially at early stages. The large number of parameters that could potentially have a significant impact on the chromatographic separation performance requires extensive experimentation traditionally performed at bench-scale in order to optimise the operating conditions. Moreover, extensive experimentation also requires a substantial amount of clarified material and long timelines [1]. High-throughput experimentation (HTE) has emerged as a powerful technique to accelerate process development with relatively small amounts of feedstock material. Nevertheless, HTE has highlighted the impetus for high-throughput analytics and the development of data manipulation and analysis tools to cope with the large datasets and leverage sufficiently the resulting information [2]. The overall aim of this paper is the establishment of a rational and systematic high-throughput process development workflow for the purification of therapeutic antibodies that incorporates decision-support techniques to leverage high-throughput purification data.

Nowadays, the regulators, through Quality by Design (QbD) and Process Analytical Technology (PAT) initiatives, prompt manufacturers to accommodate a more systematic approach in process development and optimisation in order to define a design space and determine the impact of critical process parameters on critical quality attributes. Different strategies for the development

* Corresponding author.
*E-mail address:* s.farid@ucl.ac.uk (S.S. Farid).
[1] Currently at Ipsen, Wrexham, LL13 9UF, UK.

https://doi.org/10.1016/j.chroma.2019.03.005

of purification processes are available including *in silico* and experimental laboratory approaches. *In silico* approaches include heuristic or knowledge-based methods [3–5], and algorithmic- and model-based methods [6–8]. Lab methods often rely on high-throughput experimental methods. Hybrid methods combining high-throughput experimentation (HTE) with different in silico approaches have also been presented [9]. The following paragraphs summarise the HTE approaches as well as hybrid ones.

Currently, three micro-scale formats are employed in chromatography HTE: 1) microliter batch incubation, 2) pre-packed micropipette chromatography tips and 3) pre-packed miniature packed-bed chromatography columns. Chhatre and Titchener-Hooker proposed a route to chromatography process development using micro-scale chromatography and provided a comprehensive overview of the different formats [2]. The authors discussed the operation of different micro-scale techniques and offered recommendations on their proper use either manually or using an automated liquid handling system [2]. Lacki evaluated the limitations and the advantages that these different micro-scale techniques offer and provided guidelines based on published high-throughput screening purification data, setting out which format is more appropriate for a given kind of experimental goal [10]. The author highlighted that when using the micropipette chromatography tips and the pre-packed miniature chromatography columns, it is not possible for both the residence time and the linear velocity values to be representative of values achieved with industrial scale columns given the change in bed height. Furthermore, high-throughput data obtained using the microliter batch incubation format require a mathematical manipulation in order to provide predictions at larger scales [10].

A number of studies have been published utilising microliter batch incubation and automated liquid handling systems, to investigate different types of protein chromatographic purification [11–13] and to identify the accuracy and consistency of automated liquid handling systems [1]. Additional studies have been conducted to determine the dynamic binding capacity [14,15]. The second micro-scale format using pre-packed micropipette chromatography tips has been demonstrated with the evaluation of the purification of virus-like particles [16]. Chhatre et al. used the same micropipette chromatography tips format and 2-level full factorial DoE to evaluate the effects of pH and salt concentration on the recovery and purification of polyclonal antibodies by a mixed-mode cation exchange resin [17]. The third and last micro-scale technique available incorporates miniature packed-bed chromatography columns with bed volumes of 100, 200 and 600 μL. The miniature columns are a closer representation of a packed-bed chromatography column, in terms of geometry and flow characteristics. Wierling et al. recognised the necessity for more rapid analytical tools and utilised these miniature columns coupled with an automated liquid handling system and an analytical system to evaluate the ability of four different chromatography resins to purify monoclonal antibodies from host cell proteins [18].

Another option in chromatography process development is the combination of HTE with different approaches [9,19,20]. These include combining HTE with genetic algorithms [21,22] or mechanistic modelling [23,24] to optimise process parameters for chromatography operations. Hybrid methods offer the advantage of linking different approaches emphasising the merits while mitigating the limitations that each method offers [20].

In addition to process parameter optimisation, another crucial decision at early-stage process development is the selection of the appropriate chromatography resin for each step in the correct order in the purification train. Resin selection is a rather complex task considering different resins with a wide operating range and number of process parameters for screening. An additional complication might be that different resins can be operated under different conditions thus intensifying substantially laboratory activities for experimentation (e.g. buffer preparation).

The impetus for the development of a systematic methodology to address the challenges involved in optimal chromatography resin selection has been discussed previously (e.g. [25]). Hybrid approaches to aid both resin selection and process parameter optimisation have been presented in the literature that integrate HTE with a form of model-based optimisation [26,27].

There is an increasing trend to incorporate HTE into platforms (or workflows) that combine different tools and methods forming an HTPD strategy [28]. Through the QbD initiative, regulatory agencies suggest manufacturers to adopt an HTPD strategy in order to accelerate process development from a very early stage in a product's lifecycle and achieve a high level of product and process understanding.

Previous studies have focused mainly on individual techniques with limited examples of complete workflows integrating scale-down experimentation with DoE, MVDA and decision-making tools. In addition, a further challenge often associated with HTE is how best to leverage the large amounts of raw data generated and to evaluate trade-offs in the datasets to make decisions on optimal strategies. Recognising the limitations in terms of time and materials, this work focuses on the establishment of an HTPD workflow that combines a variety of different methods in a semi-automated manner so as to streamline screening of different cation exchange (CEX) chromatography resins and optimisation of process parameters under uncertainty.

The overall aim of this research is to identify the appropriate combination of experimental approaches and decision-support techniques, in order to provide a consistent methodology for rapid generation and analysis of chromatographic purification data. A single chromatography step is investigated rather than the complete purification train in order to provide a detailed investigation of process parameters that could impact the performance of each resin candidate. The proposed HTPD workflow suggests the use of miniature pre-packed chromatography columns coupled on an automated liquid handling system, for the rapid generation of purification data. Additionally, the integration of DoE with the fractionation diagram method [29–31] was introduced to cope with the vast amounts of data generated through HTE. Furthermore, a combination of multivariate data analysis, multi-criteria decision-making and robustness analysis was established to define a potential window of operation for the chromatographic purification of a highly aggregated antibody solution.

The paper is structured as follows. Section 2 (Materials and methods) focuses on describing the individual experimental data analysis and decision-making methods and techniques used in the HTPD workflow. An example of implementing the HTPD workflow is demonstrated in Section 3 (Results and discussion) to facilitate resin screening and process parameter optimisation for bind-and-elute ion-exchange chromatography used for intermediate antibody purification.

## 2. Materials and methods

### 2.1. Materials and equipment

A bispecific antibody was used to demonstrate the implementation of the HTPD workflow. This was produced in Chinese hamster ovary (CHO) cells and cell culture material was clarified and partially purified by MedImmune. The cell culture broth was clarified by a series of depth filters and the clarified material was further processed using a Protein A chromatography column followed by a low pH hold to inactivate any enveloped viruses. The preparation of the feedstock material for the investigation of the CEX chromatography

Please cite this article in press as: C. Stamatis, et al., High throughput process development workflow with advanced decision-support for antibody purification, J. Chromatogr. A (2019), https://doi.org/10.1016/j.chroma.2019.03.005

step was completed with the neutralisation of the low pH antibody solution. All chemicals used to prepare buffers, were provided by J.T. Baker (Avantor Performance Materials Inc., Pennsylvania U.S.A). All weight measurements were performed using a BP 3100 S balance (Sartorius, Surrey UK) while pH and conductivity were measured using a PHM220 Lab pH meter and a CDM230 conductivity meter (Radiometer Analytical, Colorado U.S.A), respectively. The antibody solution was concentrated using a tangential flow filtration system (Pall Life Sciences, Portsmouth UK) with a 30 kDa polyether sulphone membrane (Millipore, Billerica, MA).

HTE was performed using an automated liquid handling system, Freedom EVO® 200 (Tecan, Maennedorf, Switzerland) and miniature chromatography columns, pre-packed with 200 μL and 600 μL of CEX resins (Atoll GmbH, Weingarten, Germany). Eight CEX resins were used in the screening study: Poros™ XS and Poros™ HS50 (Life Technologies, California, U.S.A), Toyopearl® GigaCap S-650(S)

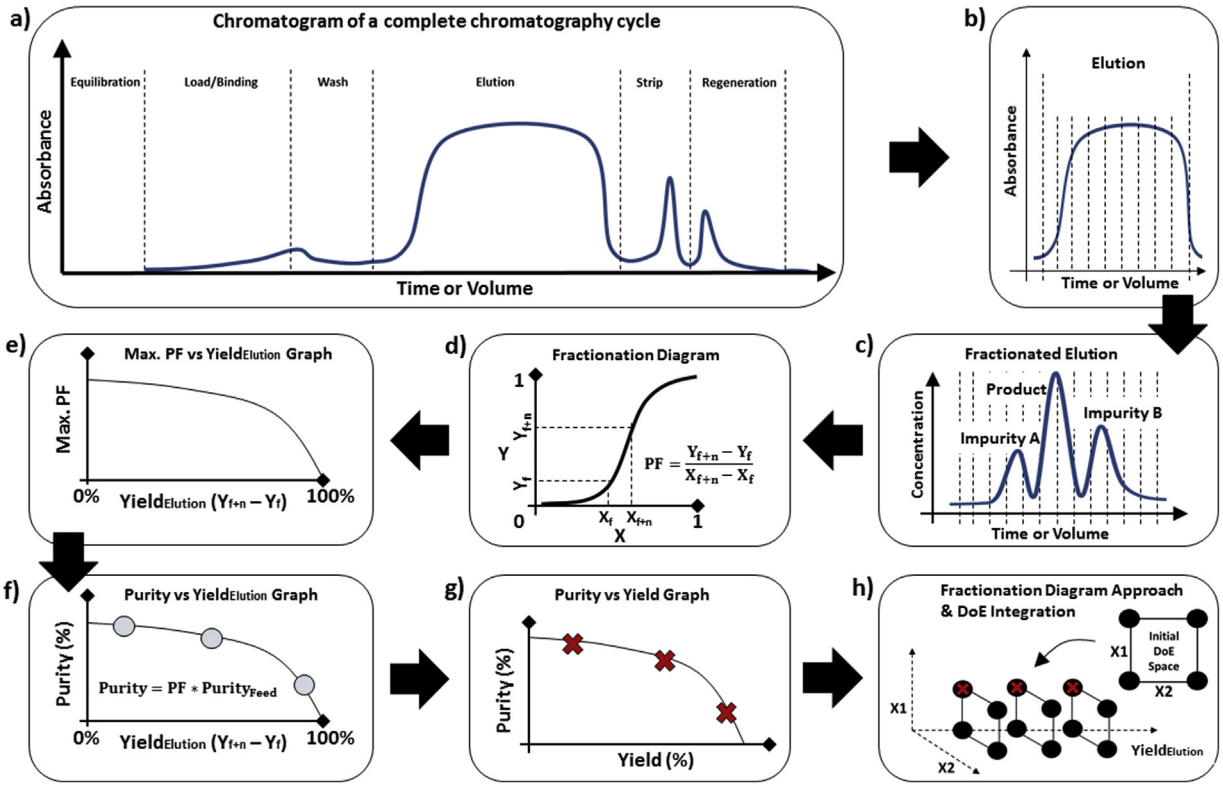


**Fig. 1.** Schematic illustration of the Fractionation Diagram methodology. a) Typical chromatogram of a complete chromatography cycle, b) Elution part of a chromatogram, c) Fractionated elution chromatogram, d) Fractionation diagram plotting the cumulative product fraction against the cumulative fraction of the total protein, e) maximum purification factor against elution yield graph, f) purity against elution yield graph, g) purity against yield graph, h) schematic illustration of the DoE – Fractionation Diagram approach integration. Steps a) through f) presented as described by Ngiam et al. [29] and steps g) & h) show the extension to the method as proposed here to account for potential product loss and integrate the method with DoE.

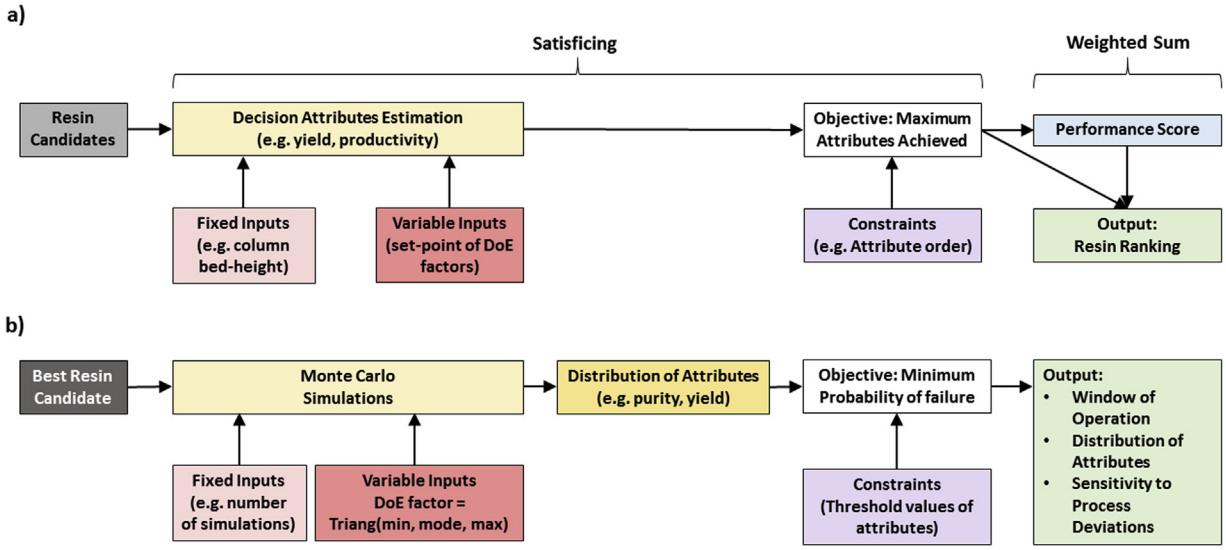


**Fig. 2.** Schematic illustration of the decision-making components of the HTPD workflow. a) Structure of the resin selection tool used to screen different resin candidates and determine the best candidate, b) Robustness analysis methodology to identify a window of operation under uncertainty.

Please cite this article in press as: C. Stamatis, et al., High throughput process development workflow with advanced decision-support for antibody purification, J. Chromatogr. A (2019), https://doi.org/10.1016/j.chroma.2019.03.005

and Toyopearl® GigaCap CM-650(M) (Tosoh Biosciences, Redditch UK), Capto™ S Impact (GE Healthcare Life Sciences, Buckinghamshire, UK), Fractogel® EMD COO- (M) and Eshmuno® CPX (EMD Millipore, Darmstadt, Germany) and UNOsphere™ Rapid S (Bio-Rad Laboratories, California, U.S.A). Bench-scale experiments were conducted using an AKTA™ Avant 25 chromatography system (GE Healthcare Life Sciences, Uppsala, Sweden). Samples, throughout the experimental work, were collected in 2 mL Masterblock® 96 deep well plates (Greiner Bio-One, Stonehouse, UK) and concentration was measured using an Xpose™ UV/VIS spectrophotometer (Trinean, Ghent, Belgium). Sample composition in terms of aggregates, product and fragments was determined using an Acquity™ UPLC system (Waters, Milford, Massachusetts, USA) with a size exclusion chromatography column with the following specifications: BEH200 with 200 A, D = 4.6 mm, L = 150 mm and 1.7 μm bead size.

### 2.2. Experimental & data analysis methodology

#### 2.2.1. Design of experiments

Screening experimentation was based on definitive screening designs while for the optimisation purposes central composite designs were used. Central composite designs have been widely employed in optimisation of chromatography systems [32–34]. On the other hand, definitive screening designs were introduced in 2011 [35] and yet have limited published examples in bioprocessing. Jones and Nachtsheim identified limitations of resolution III and IV fractional factorial designs used for early-stage screening experimentation and proposed a new class of screening designs known as definitive screening designs [35]. The proposed new class of screening designs estimates main effects completely independent of two-factor interactions. Moreover, the evaluation of each factor at three levels offers the ability to estimate quadratic effects orthogonal to main effects and not completely confounded with second order interactions. Tai et al. implemented a hybrid approach combining HTE using an ambr250™ system with a 10-factor definitive screening design for the characterisation of fermentation processes for therapeutic proteins and reported the ability of their model to capture efficiently main and quadratic effects along with higher order interactions [36].

The construction and the evaluation of the DoE space were performed in JMP Pro 11 (SAS Institute Inc., Marlow, UK) which offers a definitive screening design platform. Insights gained through screening experimentation were leveraged to develop the DoE space for the subsequent optimisation study. The resin comparison and selection methodology described in Section 2.2.3.3, determines the set-point of process parameters for each resin to meet quality and performance targets. These set-point values were used as the mid-values when designing the optimisation experiments. Having completed the experimental runs the DoE responses were estimated in MS Excel and recorded in JMP to enable the initiation of the DoE analysis. Using the Model Fit platform in JMP, a stepwise regression fitting approach was followed considering all possible main and quadratic effects and second order interactions. The stepwise regression platform in JMP follows a methodology demonstrated by Kumar et al. [34] to identify the appropriate empirical model avoiding under- or over-fitting issues using a series of standard statistical criteria (e.g. Akaike information criterion (AIC), Bayesian information criterion (BIC), $R^2$, adjusted $R^2$ and p-value threshold (<0.05)).

#### 2.2.2. Experimental set-up

For the estimation of the $DBC_{10\%}$, the flow-through volume was fractionated into fractions of equal volume (200 μL) and collected in 96-deep well plates for further analysis to determine the total protein concentration in each fraction. To evaluate selectivity and recovery, the elution pool was fractionated and each fraction (200 μL) was analysed to determine its total protein concentration and purity. Several steps were involved in the experimental set-up to investigate the dynamic binding capacity as well as the capability for purification and recovery. The process cycle started with equilibration of the chromatography matrices at the appropriate pH and conductivity conditions. Then to evaluate the binding capacity, each resin was challenged at a high load mass. For the stepwise elution experiments, equilibration was followed by loading of the product to a specific load challenge expressed as a fraction of the maximum $DBC_{10\%}$. Product and impurities were eluted with increasing conductivity of the mobile phase, followed by a high pH – high conductivity step to clean and sanitise the chromatography matrices. The same protocols were used for the purposes of subsequent steps in the HTPD workflow, to optimise the process parameters for the selected chromatography resin as well as for the model verification experiments at bench-scale. The only differences being the volume of the fractions that was collected (300 μL and 1.7 mL) and the volume of the chromatography column (600 μL and 4 mL) for the optimisation and model verification studies at bench-scale, respectively.

#### 2.2.3. Data analysis methodology

*2.2.3.1. Dynamic binding capacity at 10% breakthrough.* The $DBC_{10\%}$ was estimated using Eq. (1), where $V_{10\%}$ is the load volume (L) at 10% breakthrough, $C_{Feed}$ is the initial mAb concentration (g/L) and $V_{column}$ is the volume of the column (L) [37]. $DBC_{10\%}$ was calculated for each set of operating conditions as dictated by the DoE for screening and optimisation.

$$DBC_{10\%}(g/L) = V_{10\%}{}^{*}C_{Feed}/V_{column} \quad (1)$$

*2.2.3.2. Integration of fractionation diagram approach and design of experiments.* The execution of the experimental plan for every resin combined with the fractionation of the elution pool generated thousands of samples and hundreds of different chromatograms, posing a significant challenge in terms of sample and data analysis. To overcome the data analysis difficulties, the fractionation diagram approach was used to rapidly analyse the resulted chromatograms [29–31].

The fractionation diagram approach offers a quantitative relationship between purification and recovery. Any changes to the operating conditions such as pH or linear velocity can potentially lead to a shift to the relative position of the peaks of the product and its impurities in a chromatogram and hence to a different purification-recovery trade-off. In the fractionation diagram the Y axis (Eq. (2)) expresses the amount of product ($M_P$) collected over the total amount of product eluted, while the X axis (Eq. (3)) displays the cumulative mass fraction of the total material ($M_T$) eluted. In Eqs. (2) and (3), "F" represents the total number of fractions, "f" is the fraction index (e.g. the 3rd fraction) and "n" is the number of fractions collected in the elution pool. Therefore, any product loss during binding and wash steps in a typical chromatography cycle operating in bind-and-elute mode is ignored. Additionally, under strong binding conditions it is possible not to be able to recover the entire product during the elution step in a cycle. This issue becomes more apparent when the fractionation diagram method is used to screen a wide range of process parameters.

$$Y = \sum_{f}^{f+n} M_{P,f} / \sum_{f=1}^{F} M_{P,f} \quad \forall n \in \mathbb{N}, \quad n \le F-1 \quad (2)$$

$$X = \sum_{f}^{f+n} M_{T,f} / \sum_{f=1}^{F} M_{T,f} \quad \forall n \in \mathbb{N}, \quad n \le F-1 \quad (3)$$

Please cite this article in press as: C. Stamatis, et al., High throughput process development workflow with advanced decision-support for antibody purification, J. Chromatogr. A (2019), https://doi.org/10.1016/j.chroma.2019.03.005

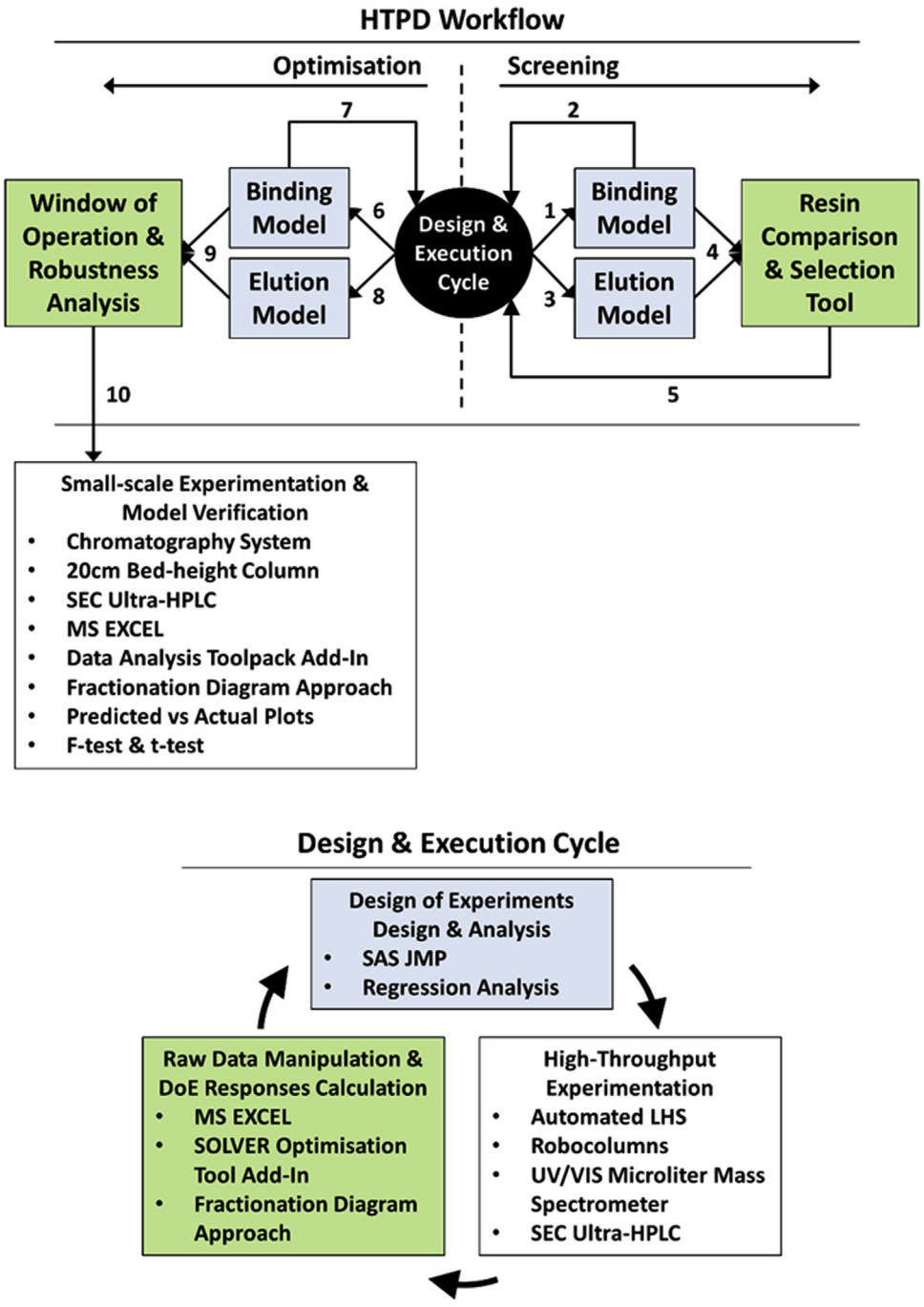


**Fig. 3.** Schematic illustration of the proposed High-Throughput Process Development workflow for a chromatography operation in bind and elute mode.

Hence, the distance between two points on the Y axis on the fractionation diagram ($Y_{f+n} - Y_f$) in this paper represents the elution yield ($Yield_{Elution}$) instead of step yield (Fig. 1d). $Yield_{Elution}$ changes from 0% to 100% regardless of the operating conditions thus ignoring any product loss. Yield can be estimated simply as the ratio of total amount of material collected in the elution pool over the total amount of material that was loaded onto the chromatography resin (Eq. (4)). To estimate yield, the total amount of material loaded is calculated as the product of $DBC_{10\%}$ and the volume of the chromatography column. The amount of product collected in the elution pool is estimated by multiplying the desired level of $Yield_{Elution}$ with the total amount of product eluted $\left(\sum_{f=1}^{F} M_{P,f}\right)$. At a certain value of $Yield_{Elution}$ there is a maximum purification factor, thus a maximum purity value (Fig. 1e). Purity is estimated as the product of the purification factor and the initial feed purity (Fig. 1f).

$$Yield\,(\%) = Yield_{Elution} * \sum_{f=1}^{F} M_{P,f} / \left(DBC_{10\%} * V_{column}\right) \quad (4)$$

Please cite this article in press as: C. Stamatis, et al., High throughput process development workflow with advanced decision-support for antibody purification, J. Chromatogr. A (2019), https://doi.org/10.1016/j.chroma.2019.03.005

*2.2.3.4. Window of operation and robust process analysis.* In cases where $\left(\sum_{f=1}^{F} M_{P,f} = M_{P,IN} = DBC_{10\%}{}^{*}V_{column}\right)$, yield would be equal to the $Yield_{Elution}$. The final step in the approach plots purity against yield (Fig. 1g). Purity is estimated as the product of the purification factor and the initial feed purity (Fig. 1f). Additionally, every purity-yield pair corresponds to a set of $Y_{f+n} - Y_f$ and $X_{f+n} - X_f$ values that define the cut-points on the respective chromatogram and thus determines the volume of the elution pool that delivers that purity-yield pair. The difference with the method initially proposed by Ngiam et al. [29] is that using the current terminology the final graph would be purity against $Yield_{Elution}$ (Fig. 1f) thus potentially overestimating the recovery capabilities of a resin at a certain set of operating conditions. Using the Purity versus Yield graph (Fig. 1g) as discussed here, a series of purity-yield pairs can be selected as dictated by the DoE space thus integrating the fractionation diagram approach with DoE (Fig. 1h). Fig. 1 shows a simplified example of the integration of the fractionation diagram approach with a two factor, two level DoE. The steps a) to f) in Fig. 1 illustrate the fractionation diagram approach as described by Ngiam et al. [29] while steps g) and h) visualise the integration of purity-yield pairs with DoE using the $Yield_{Elution}$ term as an additional factor in the DoE.

The integration of the fractionation diagram approach with DoE requires meticulous calculations to estimate the DoE responses (e.g. purity and yield). Considering also the large number of chromatograms resulted from a resin screening study the raw data manipulation becomes extremely challenging and prone to error. Nevertheless, the well-defined mathematical structure of the fractionation diagram approach allows for the development of a tool to automate the analysis. Here, for the purpose of this research, the fractionation diagram approach was programmed in MS Excel. The GRG Nonlinear engine of SOLVER (optimisation tool add-in) was called through VBA to estimate the purification factors at different $Yield_{Elution}$ values (0–100%). Furthermore, a procedure was written in VBA to automate the analysis of multiple chromatograms and for multiple resins.

*2.2.3.3. A decision-support tool for resin comparison and selection for a single chromatography step.* Statistical analysis of the DoE space for each resin candidate develops a regression model that describes each attribute (or DoE response) as a function of the process parameters (or DoE factors). Apart from screening for significant process parameters, the purpose of screening different chromatography resins is also to compare them and identify those with the greatest performance. To standardise and automate the resin comparison and selection procedure a decision-support tool was developed in MS Excel using the Solver Optimisation tool add-in with the evolutionary engine activated. The evolutionary engine receives variable inputs and searches different combinations of them to achieve the objective function while satisfying a set of constraints. A generalised schematic of the structure of the resin selection decision-support tool is presented in Fig. 2a.

A record of resin candidates included in the study is created. The resin selection tool identifies each resin using an index (i) assigned to it in order to recognise its associated fixed and variable parameters. The set-point value of the DoE factors investigated in the screening study are used as the variable inputs in the tool. Fixed inputs include the limits of the DoE factors and the regression coefficients of model parameters describing DoE responses. The DoE analysis results in a multiple linear regression (MLR) equation estimating a DoE response as a function of the DoE factors. Additional assumptions required for the calculation of key metrics included in the resin selection tool are considered as fixed inputs. For instance, to calculate productivity it is necessary to estimate the processing time thus assuming a column bed-height and the number of column volumes for each step in a chromatography cycle. Furthermore, threshold values are assigned for the decision attributes included in the resin selection tool along with their respective weight coefficient. The weight coefficient of each attribute defines its relative importance among the other attributes and therefore, dictates its priority order in the tool.

The resin selection tool operates in two stages. The first stage identifies decision attributes (e.g. yield, purity) and their relative significance and prioritises them in descending order. Thus the most important attribute is evaluated first while the least significant attribute is considered last. The evolutionary engine is searching for the set-point of process parameters (variable inputs) to achieve the threshold value for the first decision attribute. Once this is achieved the search continues with the second decision attribute while still satisfying the previous attribute. The procedure continues for all decision attributes included in the analysis with the last attribute requiring the satisfaction of all previous criteria. This approach of satisfying criteria, also known as satisficing, can potentially exclude resin candidates that meet a significant number of criteria but however fail to reach an important decision criterion that was ranked high in the priority order. Hence, it is crucial that the appropriate weight coefficients are assigned to the decision attributes in order to capture specific requirements from the resin candidates and avoid selecting resins that meet less significant criteria.

The evolutionary engine runs with the objective to maximise the number of decision attributes achieved in their respective priority order for each resin candidate while managing to meet the constraints. A set of constraints is also applied for each resin candidate in the resin selection tool to limit the variation of process parameters within the desired range. The lower and upper limits of process parameters are dictated by the DoE and considered as fixed inputs. The role of the constraints is to ensure that variable inputs fall within the acceptable range and set the threshold value for each decision attribute.

A number of resin candidates could potentially achieve all decision attributes due to either relatively low threshold values or their adequate performance. Additionally, resin selection would be difficult when resin candidates perform very similarly. To address these issues a second stage in the resin selection tool is used to assign a score to each resin candidate that successfully meets all decision attributes. A performance score is estimated for each successful resin candidate using the weighted sum method combining all the attributes used in the first stage of the tool. In Eq. (5), $w_j$ is the weight coefficient of each attribute (j), "J" is the total number of attributes and $K_i$,j is the normalised value of attribute (j) for resin (i). In case an attribute needs to be maximised in Eq. (5).1 the worst and best normalised values correspond to the minimum and maximum values of the attribute, respectively. On the other hand, in case an attribute needs to be minimised, worst and best refer to the maximum and minimum value, respectively. The term $k_{j,i}$ in Eq. (6) represents the actual value achieved of attribute (j) for resin (i).

$$\text{Performance} \quad \text{Score}_i = \sum_{j=1}^{J} w_j * K_{i,j} \tag{5}$$

$$K_{i,j} = \left(k_{i,j} - k_{i,j,worst}\right) / \left(k_{i,j,best} - k_{i,j,worst}\right) \tag{6}$$

The final decision regarding the selection of the most suitable resin candidate(s) is performed by identifying the candidate that reached the highest number of decision attributes and achieved the maximum performance score in this order. Hence, the comparison based on the score is only taking place when more than one resin candidates achieve the same maximum number of decision criteria.

Please cite this article in press as: C. Stamatis, et al., High throughput process development workflow with advanced decision-support for antibody purification, J. Chromatogr. A (2019), https://doi.org/10.1016/j.chroma.2019.03.005

The resin selection tool suggests the most suitable resin candidate(s) and also provides the set-point values for the process parameters included in the regression model that describes the factors-response relationship. These set-point values were used as the centre point in the subsequent central composite design so as to optimise process parameters and identify a window of operation. Response surface analysis of the DoE space as constructed by the central composite designs enabled the development of a set of MLR equations that describe the relationship between factors and responses. The appropriate MLR model for each response is identified using the stepwise regression approach through the Model Fit platform in JMP with a minimum BIC model selection criterion, backward elimination and a p-value threshold of 0.05.

To identify a window of operation that satisfies a number of quality and performance attributes a stochastic simulation engine was built in MS Excel (Fig. 2b). Each process parameter was expressed using a triangular distribution defined by its mode, minimum and maximum values representing the set-point and its deviation limits. The resulting probabilistic process parameters were then used to estimate each DoE response (e.g. purity, yield) using the MLR correlations developed through the optimisation study for the selected resin candidate. A series of Monte Carlo simulations were performed by varying the set-point and its deviation limits for each process parameter and deriving distributions for each DoE response. An optimisation was set up to determine the optimal set-point and range that minimised the objective function. This was achieved using the evolutionary engine provided by the SOLVER optimisation tool add-in in MS Excel, which was set to receive the set-point and its deviation limits for each process parameter (DoE factors) as decision variables. The objective function was defined as minimisation of the probability of process failure. In this context process failure was considered the probability of failing to meet the threshold value for any of the quality and performance attributes. For instance, assuming two attributes of purity and yield, the probability of process failure is defined as [38]:

$$P(\text{fail}) \equiv P(A \cup B) = P(A) + P(B) - P(A \cap B) \quad (7)$$

where:

$$P(A) = \sum_{1}^{N} E(A)/N \quad (8)$$

$$P(B) = \sum_{1}^{N} E(B)/N \quad (9)$$

E(A): the event where purity fails to meet the threshold purity value

E(B): the event where yield fails to meet the threshold yield value

P(A): the probability of failing to meet the threshold purity value

P(B): the probability of failing to meet the threshold yield value

P(A∩B): the probability of failing both purity and yield threshold values

N: Total number of simulations (sample space)

A potential window of operation is defined by a set-point (mode) value and an acceptable range (min., max.) for each process parameter (DoE factor) in order to minimise the probability of process failure. The robustness of the optimal solution as defined by SOLVER was further analysed by examining its associated Monte Carlo simulation dataset to determine the parameters with the greatest impact on each attribute and visualise its distribution using @RISK (Palisade Corporation, NY, USA).

#### 2.2.4. Bench-scale model verification

To verify the predictive ability of the model, targeted experimentation within the suggested window of operation was performed at bench-scale using a self-packed chromatography column with a bed-height of 20 cm and a diameter of 0.5 cm. The sequence and configuration of the chromatography cycle was similar to that used at micro-scale with the only difference being the gradient elution profile. Experimentation related to the HTPD workflow was conducted with a stepwise elution profile due to limitations related with the liquid handling system. On the other hand, experimentation at bench-scale was performed by applying a linear conductivity gradient profile so as to enable a more accurate determination of the conductivity range where product is collected in the elution pool. Experimentally achieved values (or actual values) were plotted against predicted values for each attribute to visualise the accuracy of the predictions. Additionally, statistical tests (F-test and t-test) were performed to address the hypothesis that actual and predicted values are all from the same distribution comparing the mean and standard deviation for each dataset.

## 3. Results & discussion

The previous section described the individual components of the HTPD workflow and highlighted its capability to adapt to different user specifications. This section focuses on presenting the implementation of the workflow for a particular purification challenge and demonstrating the linkage among different components of the workflow.

A case-study was formulated in collaboration with MedImmune to demonstrate the HTPD workflow, using a bispecific monoclonal antibody with high aggregate concentration post Protein A chromatography. The main steps involved in the HTPD workflow are outlined in Fig. 3. The design and execution cycle is the central component of the workflow that combines DoE, the fractionation diagram method, high-throughput experimentation and multivariate data analysis. A key output of the design and execution cycle is the regression models (i.e. binding and elution models) which can be imported into decision-support tools for further evaluation. Starting with a screening study, regression models are used in the resin selection tool to determine the best resin candidate. On the other hand, an optimisation study leverages binding and elution regression models using a robustness analysis tool to identify a window of operation under uncertainty in process parameters.

### 3.1. Preparation for the HTPD workflow

It is essential to gather relevant information regarding the product and the process before proceeding into any experimental work. For instance, information on previously tested CEX chromatography resins, significant process parameters and ranges, level and composition of impurities as well as properties related to the molecule under investigation could all provide critical insights and hence promote and improve the design of the experiments. After discussion with the purification process development team in MedImmune (Granta Park, Cambridge, UK), eight CEX chromatography resins (as named in Section 2.1) were chosen to be included in the study. Due to the high aggregate concentration (20%) post Protein A chromatography, the primary consideration was the identification of resin candidates that could remove a sufficient amount of high molecular weight (HMW) species.

Additional information required is the mode of operation of the selected resin candidates. Given the high isoelectric point (>8.5) of the particular bispecific mAb, CEX chromatography resins were operated in bind-and-elute mode. A typical chromatography cycle operating in bind-and-elute mode involves six main steps: equili-

Please cite this article in press as: C. Stamatis, et al., High throughput process development workflow with advanced decision-support for antibody purification, J. Chromatogr. A (2019), https://doi.org/10.1016/j.chroma.2019.03.005

bration, load, wash, elution, strip and resin regeneration. The two steps investigated here were the load (or binding) step and the elution step. The operation conditions for resin equilibration and wash were dictated by the operating conditions for binding and elution, respectively, while a universal protocol was used to strip and regenerate all CEX resins. Binding and elution conditions were evaluated through two different sets of DoE.

### 3.2. Design and analysis of experiments

The HTPD workflow starts with the construction of the DoE space to investigate the binding conditions for each CEX resin. A definitive screening design was created in JMP with four continuous factors (process parameters) and a single response (Table 1). The conditions of the mobile phase (pH and conductivity), the linear velocity and the concentration of the feed were the four factors considered in the DoE with $DBC_{10\%}$ as the only response to be maximised. Linear velocity was adjusted in order to keep the residence time between two scales constant. At micro-scale the bed-height is 1 cm and 3 cm for a 200 μL and a 600 μL miniature chromatography column, respectively while a typical bed-height at pilot- and large-scale would be around 20 cm. Thus operating a 20 cm bed-height column at a linear velocity of 300 cm/h would result in a residence time of 4 min. The corresponding linear velocity at micro-scale can be estimated by keeping constant the residence time. For this example, using a 600 μL column the linear velocity would be 45 cm/h.

The definitive screening design platform in JMP Pro 11 created a design of nine runs with four factors to screen in order to maximise the $DBC_{10\%}$ for each CEX resin. Breakthrough curves resulted from the DoE runs were analysed in MS Excel to calculate the $DBC_{10\%}$ at each set of operating conditions and for each CEX resin. $DBC_{10\%}$ values were imported in JMP and through a stepwise regression analysis, a MLR regression model was developed estimating $DBC_{10\%}$ as a function of the DoE factors and for each CEX resin. Each model demonstrated an $R^2$ and adjusted $R^2$ value above 80% and a p-value less than 0.05 through analysis of variance (ANOVA) indicating that variability of the response from its mean value is not due to chance. A set of operating conditions that seemed to favour every CEX resin was identified in order to simplify subsequent experimentation to evaluate the elution operating conditions. Three process parameters were selected as the DoE factors (elution pH, elution linear velocity and load challenge) in the elution definitive screening design created to screen for maximum purity and yield for each CEX resin. The conductivity gradient profile of the mobile phase during elution was kept the same throughout the experimental runs and for all CEX resins. A stepwise elution profile over 20 column volumes from 0 mM to 450 mM with a 50 mM step of sodium chloride was applied.

The term load challenge expresses the binding capacity of a CEX resin as a fraction of its $DBC_{10\%}$. Additionally, the product recovery term, $Yield_{Elution}$, was considered as the fourth factor in the elution definitive screening design as discussed in Section 2.2.3.2, in order to achieve the integration of DoE and the fractionation diagram approach. Hence the resulted DoE space consisted of four factors leading to nine experimental runs investigating two responses. Two CEX resins demonstrated the lowest $DBC_{10\%}$ and therefore load challenge was not considered as a factor in their elution definitive screening design. The evaluation of all three DoE responses ($DBC_{10\%}$, purity and yield) was achieved using the resin selection tool.

### 3.3. Resin comparison and selection

The structure and the main components of the resin selection tool are illustrated in Fig. 2. Additionally, Table 2 provides a summary of its main components used in the case-study. To initiate the comparison and selection protocol it is necessary to define the desired decision attributes along with their relative importance. As discussed above, due to the high concentration of HMW species it was crucial to identify CEX resin candidates that had high HMW removal capabilities (over 70%). Therefore, HMW removal (Eq. (10)) was selected as the first decision attribute and it was assigned a weight coefficient of 40%. High HMW removal may result in product loss in cases with poor selectivity and peak resolution; thus, a second metric was introduced to evaluate the purity of the product (monomer) from HMW species. For the purposes of the screening study it is equally important to identify the best resin candidate and determine how the rest of the candidates compare. Therefore, instead of comparing the resin candidates using the purity of the bispecific antibody a different metric was introduced to capture the change in purity relative to the theoretical maximum improvement. Eq. (11) describes that change in purity which was given a weight coefficient of 30%. The third decision attribute considered was the step yield (Eq. (4)) followed by productivity (Eq. (12)) assigned a weight coefficient of 20% and 10%, respectively. The determination of the appropriate weight coefficients along with their threshold values was achieved after discussion with the purification team at MedImmune (Cambridge, UK).

$$\text{HMW}\quad \text{Removal}\ (\%) = 1 - \left(\text{HMW}_{\text{Elution pool}}/\text{HMW}_{\text{Feed}}\right) \tag{10}$$

$$\text{Purity}\quad \text{Change}\,(\%) = \frac{\left(\text{Purity}_{\text{Elution pool}} - \text{Purity}_{\text{Feed}}\right)}{\left(1 - \text{Purity}_{\text{Feed}}\right)} \tag{11}$$

$$\text{Productivity}\ \left(\text{g/L/h}\right) = \text{DBC}^{*}\text{Yield/t} \tag{12}$$

where:

$$\text{t (hours)} = \left(\frac{\text{CV}_{\text{Load}} + \text{CV}_{\text{Equilibration}}}{\text{u}_{\text{Load}}} + \frac{\text{CV}_{\text{Wash}} + \text{CV}_{\text{Elution}}}{\text{u}_{\text{Elution}}} + \frac{\text{CV}_{\text{Strip \& Regen.}}}{\text{u}_{\text{Strip \& Regen.}}}\right)^{*}\text{H} \tag{13}$$

$HMW_{Elution\ pool}$: mass of HMW species collected in the elution pool (g)

$HMW_{Feed}$: initial mass content of HMW species in the feed stream (g)

u: Linear velocity (cm/h)

CV: Number of column volumes

H: Column bed-height (cm)

t: chromatography cycle time (hours)

The resin selection tool receives these specifications by the user and organises accordingly the order that each attribute is evaluated. Then an evolutionary engine (SOLVER Optimisation tool, Excel) searches for the set-point of process parameters for each CEX to achieve threshold values of the decision attributes as shown in Table 2. The final decision was based on the weighted sum method assigning a performance score (Eq. (5)) to each CEX resin based on the value it achieved for each decision attribute (Eqs. (4), (10)–(12)). The CEX resin that met the maximum number of decision attributes and achieved the highest performance score (in that order) was selected as the most suitable candidate to undergo further experimentation to optimise its operating conditions. An illustration of the final outcome of the tool for the bispecific mAb case study is presented in Fig. 4.

Two CEX resin candidates managed to achieve all four decision criteria in their respective order. It should be noted that the yield requirement was dropped to a low level in order to allow a high HMW removal. Due to high aggregate concentration and poor peak resolution achieved with the 200 μL chromatography columns a substantial reduction of HMW species was only achieved through decreased product recovery. Although limitations were

Please cite this article in press as: C. Stamatis, et al., High throughput process development workflow with advanced decision-support for antibody purification, J. Chromatogr. A (2019), https://doi.org/10.1016/j.chroma.2019.03.005

**Table 1**
Design of Experiments used in the HTPD workflow for screening and optimisation of CEX chromatographic separation for a bispecific antibody.

| DoE | Binding | Elution |
|---|---|---|
| **Screening** | Factors<br>• Load pH (4.5–7.5)<br>• Load Conductivity (0–150 mM)<br>• Load Linear Velocity (300–500 cm/h)<br>• Feed Concentration (4 – 12 g/L)<br><br>Response<br>• $DBC_{10\%}$ (Maximise) | Factors<br>• Elution pH (5.0–7.0)<br>• Elution Linear Velocity (300–500 cm/h)<br>• Load Challenge (30–90 g/L)<br>• Elution Yield (50–100%)<br><br>Responses<br>• Purity (Maximise)<br>• Yield (Maximise) |
| **Optimisation** | Factors<br>• Load pH (4.5–5.5)<br>• Load Conductivity (0–75 mM)<br>• Load Linear Velocity (350–500 cm/h)<br><br>Response<br>• $DBC_{10\%}$ (Maximise) | Factors<br>• Elution pH (4.5–5.5)<br>• Elution Linear Velocity(300–500 cm/h)<br>• Load Challenge (40–120 g/L of resin)<br>• Elution Yield (50–100%)<br><br>Responses<br>• Purity (Maximise)<br>• Yield (Maximise)<br>• Elution Pool Volume (Minimise) |

**Table 2**
Case study formulation of the decision-making components in the HTPD workflow.

| HTPD workflow step | Resin Comparison & Selection Tool | Window of Operation & Robustness Analysis |
|---|---|---|
| **Variables**<br>**Fixed Inputs** | Set point of process parameters (DoE factors)<br>• Regression coefficients<br>• DoE factors' limits<br>• Weight of decision attributes:<br>○ $W_{HMW\ removal} = 0.4$<br>○ $W_{Purity\ change} = 0.3$<br>○ $W_{Yield} = 0.2$<br>○ $W_{Productivity} = 0.1$ | Set point & acceptable range of process parameters (DoE factors)<br>• Regression coefficients<br>• DoE factors' limits<br>• Monte Carlo runs = 10000 |
| **Constraints** | • $DBC_{10}\%$ > Load Challenge<br>• Variables within limits<br>• Prioritised attribute targets:<br>1 HMW removal ≥ 70%<br>2 Purity change ≥ 50%<br>3 Yield ≥ 50%<br>4 Productivity ≥ 25 g/L/h | • Variables within limits<br>• Attributes' threshold values:<br>○ DBC10% ≥ 110 g/L<br>○ Purity ≥ 91%<br>○ Yield ≥ 75%<br>○ Pool volume ≤ 5CV |
| **Objective**<br>**Outcome** | Maximum: Number of achieved decision attributes in priority order<br>• Resin Ranking<br>• Set-point of process parameters<br>• Selected Resin | Minimum: Probability of process failure P(fail)<br>• Window of Operation<br>• Distribution of attributes<br>• Sensitivity to process deviations |

observed regarding the use of the 200 μL miniature columns (e.g. flowrate limitations of the robotic arm and poor peak resolution due to the small bed-height), they were universal for all CEX resins. Therefore, for comparability purposes the 200 μL chromatography columns were considered sufficient providing the advantage of low material consumption especially when multiple CEX resins are screened.

Between the two successful CEX resin candidates the performance score achieved by Resin-7 was approximately 85% compared to 55% achieved by Resin-1. Hence, Resin-7 was determined as the top-ranked CEX resin that was selected to undergo further experimentation to optimise its operating conditions. Fig. 4 also provides a ranking of all the CEX resins included in screening. Additionally, the set-points of the operating parameters for each CEX resin are shown in Fig. 4. Given the configuration of the resin selection tool for the particular bispecific mAb, the majority of the CEX resins managed to remove HMW species and increase purity. However, a low level of yield was observed throughout all resin candidates that partially rendered them incapable of reaching the productivity target.

### 3.4. Window of operation

Leveraging the CEX resin screening results summarised in Fig. 4, the subsequent optimisation experiments were designed for the selected Resin-7 (Table 1). It should be noted that binding conditions were optimised considering only to maximise $DBC_{10\%}$. On the other hand, the elution pool volume that was collected was introduced as the third DoE response after purity and yield due to its impact on productivity. A stepwise regression analysis identified a model to describe each of the four DoE responses as a function of the DoE factors. Fig. 5 shows the prediction profilers of each DoE response along with a model-fit summary.

Instead of using the prediction profilers to identify a sweet spot, the MLR coefficients were linked into a stochastic simulation engine evaluating simultaneously the set-point and the acceptable range of each process parameter. Through a series of Monte Carlo simulations a window of operation was determined where the probability of failing to meet the threshold values of any attribute is minimised. The contour plots in Fig. 6 demonstrate the areas where all attributes are satisfied (white areas) operating under no devia-

Please cite this article in press as: C. Stamatis, et al., High throughput process development workflow with advanced decision-support for antibody purification, J. Chromatogr. A (2019), https://doi.org/10.1016/j.chroma.2019.03.005

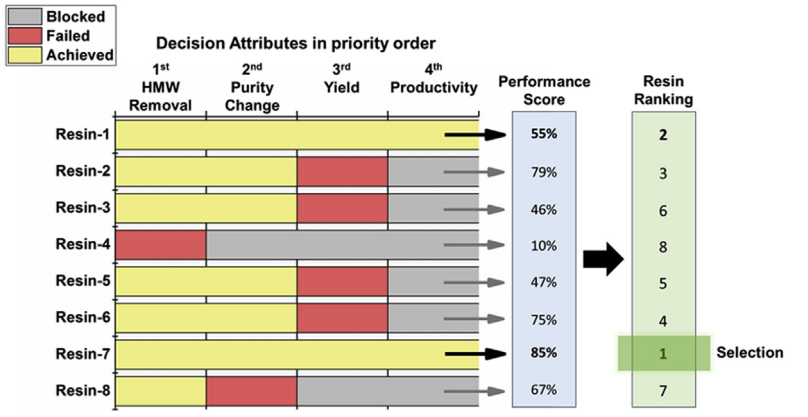


| CEX Chromatography Resin | R1 | R2 | R3 | R4 | R5 | R6 | R7 | R8 |
|---|---|---|---|---|---|---|---|---|
| pH - Load | 4.9 | 4.5 | 4.8 | 4.8 | 4.9 | 5.6 | 4.9 | 4.5 |
| Conductivity - Load (mM) | 54 | 36 | 3 | 60 | 101 | 4 | 35 | 0 |
| Linear Velocity - Load (cm/h) | 402 | 366 | 418 | 395 | 388 | 409 | 421 | 300 |
| Feed Concentration (g/L) | 12.0 | 9.3 | 8.8 | 7.2 | 5.2 | 7.2 | 12.0 | 4.0 |
| pH – Elution | 5.5 | 6.9 | 7.0 | 5.0 | 6.2 | 5.8 | 5.1 | 5.0 |
| Linear Velocity - Elution (cm/h) | 450 | 368 | 300 | 448 | 354 | 334 | 498 | 300 |
| Load Challenge (g/L) | 80 | 45 | 31 | 35 | 35 | 30 | 90 | 30 |

**Fig. 4.** A visualisation of the resin selection tool developed to identify CEX resins that meet the desired decision attributes. User specifications define the priority order of the decision attributes. Achieved attributes are determined using the satisficing method. Each resin candidate is assigned a performance score combining their respective attribute normalised values. Ranking is performed considering first the resin candidates with the highest number of achieved attributes and then their performance score. The set-point of each process parameter is presented in the table. CEX resin in order of appearance 1–8: Poros XS, Poros HS 50, Toyopearl GigaCap S 650 (S), Toyopearl GigaCap CM 650 (M), Capto S Impact, Fractogel COO (M), Eshmuno CPX and UNOsphere Rapid S.

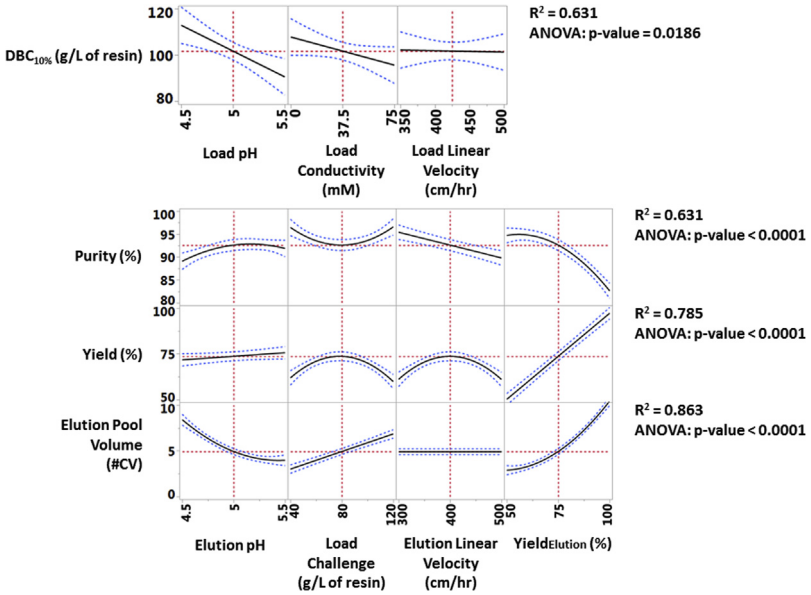


**Fig. 5.** Prediction profilers generated using JMP Pro 11 to visualise each attribute (DoE response) as a function of process parameters (DoE factors) for CEX Resin – 7. Solid lines represent the average response and dotted lines indicate the confidence interval at a 95% confidence level.

tions from the set-point. Additionally, black shaded circular areas present the window of operation considering a level of uncertainty for each process parameter.

Typically, a window of operation would focus on defining the boundaries of an operating space and determine its centre point as the sweet-spot due to its greatest distance from the boundaries and thus potentially increasing the robustness of a process. Although this approach defines the set-point for each process parameter, it neglects to determine an acceptable range within which each process parameter is allowed to vary without compromising any quality and performance attributes. Additionally, when multiple parameters are investigated a series of contour plots would be necessary to describe a window of operation especially when parameter interactions have a significant impact on the attributes. Using the methodology as described in Section 2.2.3.4, it is possible to determine an acceptable operating range for each process parameter along with its set-point. Thus providing a greater understanding regarding the impact of process parameters on different attributes and hence guide subsequent experimentation at larger scales.

Using the Monte Carlo simulations dataset, which resulted in a minimum probability of process failure, a distribution for each

Please cite this article in press as: C. Stamatis, et al., High throughput process development workflow with advanced decision-support for antibody purification, J. Chromatogr. A (2019), https://doi.org/10.1016/j.chroma.2019.03.005

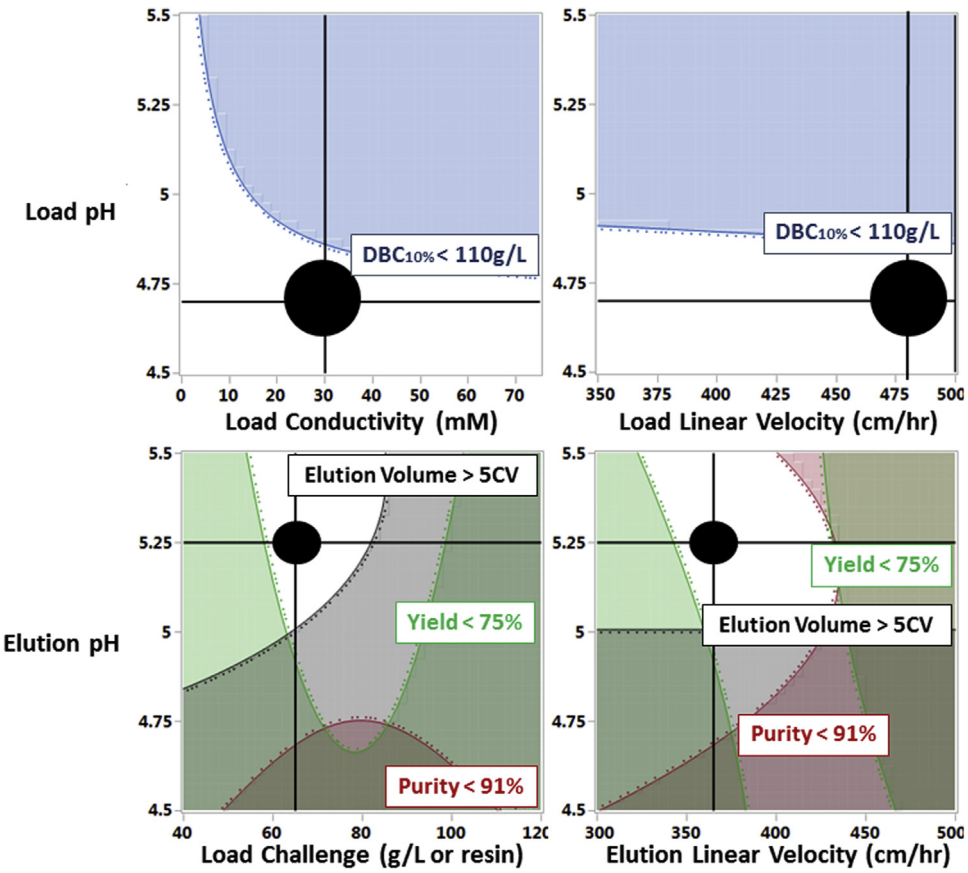


**Fig. 6.** Window of operation under uncertainty for CEX Resin – 7. White (blank) areas demonstrate the operating space under no process deviations from the set-point. Black areas define a window of operation that satisfies the attributes under uncertainty by minimising the probability of failing any of the threshold values of the attributes.

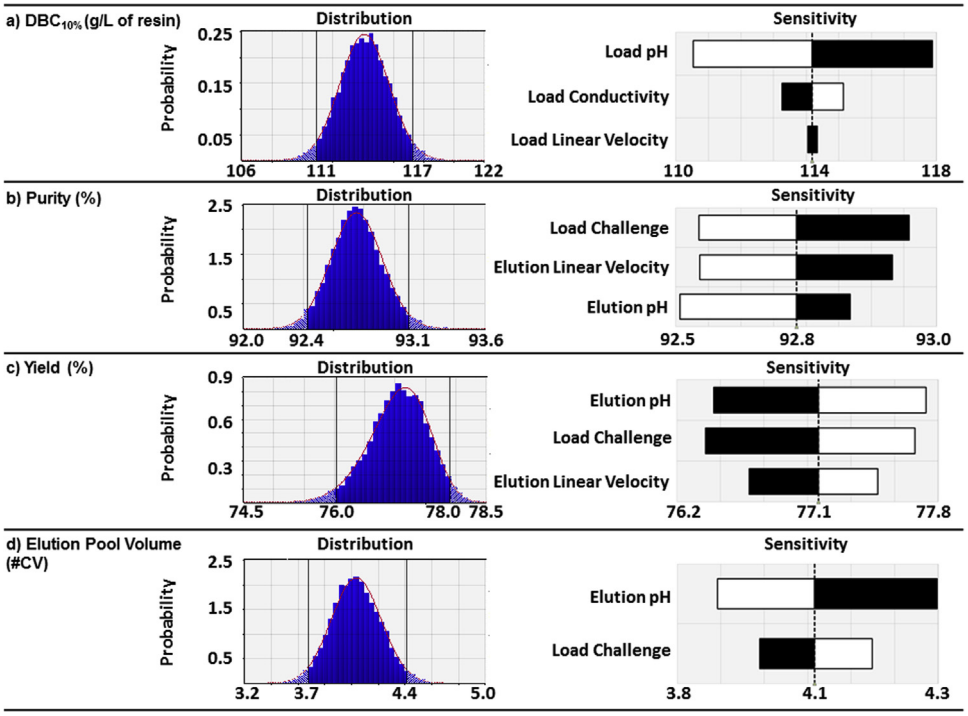


**Fig. 7.** Robustness analysis for CEX Resin – 7. Distribution and sensitivity of attributes operating with the identified window of operation under uncertainty. Solid bars in the tornado graphs for the sensitivity analysis indicate lower parameter values than the set-point and hollow bars indicate higher value.

Please cite this article in press as: C. Stamatis, et al., High throughput process development workflow with advanced decision-support for antibody purification, J. Chromatogr. A (2019), https://doi.org/10.1016/j.chroma.2019.03.005

attribute was created and a tornado plot was drawn to evaluate the significance of each process parameter (Fig. 7). The process parameter with the most significant impact on $DBC_{10\%}$ was identified as the load (binding) pH, while all operating parameters demonstrated an impact on purity and yield. It should be noted that it can be expected that the linear velocity of the mobile phase during elution would have no effect on the volume of the elution pool as can be seen in Figs. 5–7.

Furthermore, the benefits of using the 600 μL miniature chromatography columns should be highlighted as it was possible to achieve a greater peak resolution compared with the 200 μL columns. That led to a more realistic approximation of the trade-offs between purity and yield.

### 3.5. Targeted bench-scale experimentation

The validity of the predictions made through the implementation of the HTPD workflow was assessed by performing targeted experiments at bench-scale with a 20 cm bed-height chromatography column packed with Resin-7. Bench-scale experimentation evaluated the operation at the centre of the suggested window of operation (set-point of process parameters) while additional runs were performed deliberately introducing deviations from the set-point within and outside the window of operation.

The $DBC_{10\%}$ was evaluated first in order to determine whether the predicted value of load challenge was feasible. Experimentally achieved (i.e. actual) $DBC_{10\%}$ values were plotted against predicted to visualise their accuracy. It can be noted that $DBC_{10\%}$ was consistently overestimated leading to a shift of the data-points in Fig. 8a from the diagonal line to the right. In order to improve the accuracy of the predictions, the predicted $DBC_{10\%}$ was corrected to account for the collection of a column volume of equilibration buffer in the flow-through pool at the beginning of the loading phase and the hold-up mass with the application of the last column volume (Eq. (14)). Additional breakthrough curves were generated to address the validity of the correction made (Fig. 8b).

$$DBC_{10\%}^{Corrected} = DBC_{10\%}^{Predicted} - 2^{*}C_{Feed} \quad (14)$$

Linear gradient elution experiments followed to evaluate the predictive ability of the elution performance at bench-scale. Experimental values were plotted against predicted for each attribute (purity, yield and elution pool volume) as shown in Fig. 8c–e. Statistical tests were performed to assess the significance of the difference between the means (*t*-Test) and the variances (F-Test) of the predicted and the actual values. The test results suggested a good agreement between the predicted and the experimental values for purity and yield while there was a statistically significant difference between the variances of the predicted and the actual datasets on elution pool volume. Additionally, the over-prediction of the $DBC_{10\%}$ without the application of the correction for the hold-up mass was confirmed. A potential source of error leading to the over-prediction of DBC could be the capacity of the pipettes in the robotic arm of the liquid handling system. When the load volume exceeds the maximum volume of the pipettes of the robotic arm, multiple aspiration/dispersion cycles are required. In such cases, the delay of the robotic arm would increase the residence time that could cause a surge in DBC. Hence, for future studies the delay of the robotic arm should be quantified and considered for the calculation of the flowrate at micro-scale.

In summary, implementation of the proposed HTPD workflow enabled the comparison of a number of CEX resins under conditions that favour each candidate. Two CEX resins qualified as suitable candidates for this particular purification challenge. The CEX Resin-7 was selected based on its performance score for further experimentation to identify a window of operation. The results suggested a mean predicted purity and yield level of 93% and 76%, respectively with an elution pool volume of 4.0 CV. Targeted bench-scale experimentation within the predicted window of operation

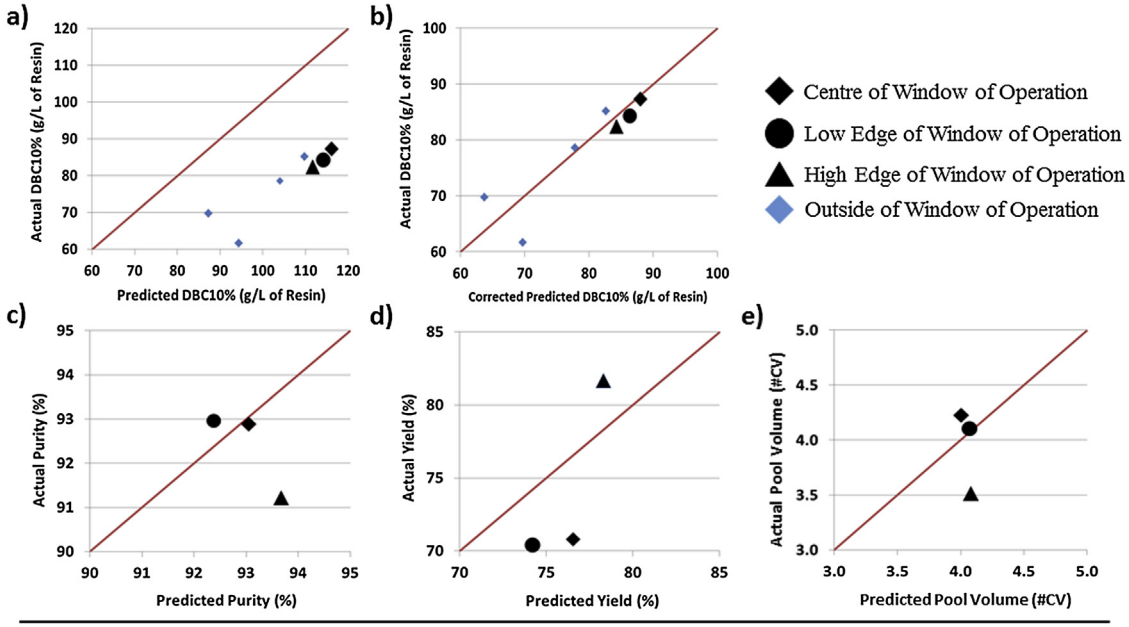


| | a | b | c | d | e |
|---|---|---|---|---|---|
| F-test: p-value | 0.37 | 0.47 | 0.30 | 0.09 | 0.01 |
| t-test: p-value | 0.0003 | 0.92 | 0.39 | 0.65 | 0.68 |

**Fig. 8.** Actual vs Predicted plots and Statistical tests to visualise and verify the proposed window of operation for CEX Resin – 7. The null hypothesis considers the two samples sets are from the same distribution. P-values ≤ 0.05 reject the null hypothesis.

Please cite this article in press as: C. Stamatis, et al., High throughput process development workflow with advanced decision-support for antibody purification, J. Chromatogr. A (2019), https://doi.org/10.1016/j.chroma.2019.03.005

resulted in similar performance (92% purity, 74% yield and 3.9 CV) and hence provided a preliminary justification of the predictive ability of the model.

## 4. Conclusions

This paper demonstrated the implementation of a novel high-throughput process development (HTPD) workflow for the chromatographic purification of a highly aggregated bispecific monoclonal antibody (mAb). The HTPD workflow linked high-throughput experimentation (HTE) at micro-scale with design of experiments (DoE), regression analysis, multi-attribute decision-making and stochastic analysis. A key focus of the HTPD workflow was the establishment of a systematic framework providing the methods and the tools to cope with the large datasets resulting from HTE and automate a significant part of data manipulation and analysis. Insights gained throughout the implementation of the HTPD workflow can be further leveraged to guide experimentation at larger scales towards the establishment of a design space and a control strategy.

## Acknowledgements

Financial support from the UK Engineering and Physical Sciences Research Council (EPSRC) (grant reference number: EP/G034656/1) and MedImmune Ltd (a member of the AstraZeneca Group) is gratefully acknowledged. Constructive feedback and technical advice from industrial experts at MedImmune is gratefully acknowledged, in particular from the downstream process development team in Cambridge UK. UCL Biochemical Engineering hosts the Future Targeted Healthcare Manufacturing Hub in collaboration with UK universities and with funding from the UK Engineering & Physical Sciences Research Council (EPSRC) and a consortium of industrial users and sector organisations.

## References

[1] J.L. Coffman, J.F. Kramarczyk, B.D. Kelley, High-throughput screening of chromatography separations: I. Method development and column modeling, Biotechnol. Bioeng. 100 (2008) 605–618.
[2] S. Chhatre, N.J. Titchener-Hooker, Review: microscale methods for high-throughput chromatography development in the pharmaceutical industry, Chem. Eng. Technol. 84 (2009) 927–940.
[3] S.M. Wheelwright, The design of downstream processes for large-scale protein purification, J. Biotechnol. 11 (1989) 89–102.
[4] J.A. Asenjo, L. Herrera, B. Byrne, Development of an expert system for selection and synthesis of protein purification processes, J. Biotechnol. 11 (1989) 275–298.
[5] E.W. Leser, J.A. Asenjo, Rational design of purification processes for recombinant proteins, J. Chromatogr. 584 (1992) 43–57.
[6] T. Gu, G.J. Tsai, G.T. Tsao, New approach to a general nonlinear multicomponent chromatography model, AIChE J. 36 (1990) 784–788.
[7] G. Guiochon, Preparative liquid chromatography, J. Chromatogr. A 965 (2002) 129–161.
[8] S. Chan, N. Titchener-Hooker, D.G. Bracewell, E. Sorensen, A systematic approach for modeling chromatographic processes – application to protein purification, AIChE J. 54 (2008) 965–977.
[9] B.K. Nfor, T. Ahamed, G.W. van Dedem, E.J. van de Sandt, M.H. Eppink, Design strategies for integrated protein purification processes: challenges, progress and outlook, J. Chem. Technol. Biotechnol. 83 (2008) 124–132.
[10] K.M. Lacki, High-throughput process development of chromatography steps: advantages and limitations of different formats used, Biotechnol. J. 7 (2012) 1192–1202.
[11] J.F. Kramarczyk, B.D. Kelley, J.L. Coffman, High-throughput screening of chromatography separations: II. Hydrophobic interactions, Biotechnol. Bioeng. 100 (2008) 707–720.
[12] B.D. Kelley, S.A. Tobler, P. Brown, J.L. Coffman, R. Godavarti, T. Iskra, M. Switzer, S. Vunnum, Weak partitioning chromatography for anion exchange purification of monoclonal antibodies, Biotechnol. Bioeng. 101 (2008) 553–566.
[13] B.D. Kelley, M. Switzer, P. Bastek, J.F. Kramarczyk, K. Molnar, T. Yu, J. Coffman, High-throughput screening of chromatography separations: IV. Ion-exchange, Biotechnol. Bioeng. 100 (2008) 950–963.
[14] T. Bergander, K. Nilsson-Valimaa, K. Oberg, K.M. Lacki, High-throughput process development: determination of dynamic binding capacity using microtiter filter plates filled with chromatography resin, Biotechnol. Prog. 24 (2008) 632–639.
[15] G. Catra, Predicting protein dynamic binding capacity from batch adsorption tests, Biotechnol. J. 7 (2012) 1216–1220.
[16] M.D. Wenger, P. DePhillips, C.E. Price, D.G. Bracewell, An automated microscale chromatographic purification of virus-like particles as a strategy for process development, Biotechnol. Appl. Biochem. 47 (2007) 131–139.
[17] S. Chhatre, D.G. Bracewell, N.J. Titchener-Hooker, A microscale approach for predicting the performance of chromatography columns used to recover therapeutic polyclonal antibodies, J. Chromatogr. A 1216 (2009) 7806–7815.
[18] P.S. Wierling, R. Bogumil, E. Knieps-Grunhagen, J. Hubbuch, High-throughput screening of packed-bed chromatography coupled with SELDI-TOF MS analysis: monoclonal antibodies versus host cell protein, Biotechnol. Bioeng. 98 (2007) 440–450.
[19] B.K. Nfor, P.D. Verhaert, L.A. Wielen, J. Hubbuch, M. Ottens, Rational and systematic protein purification process development: the next generation, Trends Biotechnol. 27 (2009) 673–679.
[20] A.T. Hanke, M. Ottens, Purifying biopharmaceuticals: knowledge-based chromatographic process development, Trends Biotechnol. 32 (2014) 210–220.
[21] A. Susanto, K. Treier, E. Knieps-Grunhagen, E.V. Lieres, J. Hubbuch, High throughput screening for the design and optimisation of chromatographic processes: automated optimisation of chromatographic phase systems, Chem. Eng. Technol. 32 (2009) 140–154.
[22] K. Treier, P. Laster, J. Hubbuch, Application of genetic algorithms and response surface analysis for the optimisation of batch chromatographic systems, Biochem. Eng. J. 63 (2012) 66–75.
[23] A. Osberghaus, K. Drechsel, S. Hansen, S.K. Hepbildikler, S. Nath, M. Haindl, E. von Lieres, J. Hubbuch, Model-integrated process development demonstrated on the optimisation of a robotic cation exchange step, Chem. Eng. Sci. 76 (2012) 129–139.
[24] S.J. Traylor, X. Xu, Y. Li, M. Jin, Z.J. Li, Adaptation of the pore diffusion model to describe multi-addition batch uptake high-throughput screening experiments, J. Chromatogr. A 1368 (2014) 100–106.
[25] A.S. Rathore, Resin screening to optimize chromatographic separations, LCGC 19 (2001) 616–622.
[26] B.K. Nfor, D.S. Zuluaga, P.J.T. Verheijen, P.D.E.M. Verhaert, L.A.M. van der Wielen, M. Ottens, Model-based rational strategy for chromatographic resin selection, Biotechnol. Prog. 27 (2011) 1629–1643.
[27] S. Liu, S. Gerontas, D. Gruber, R. Turner, N.J. Titchener-Hooker, L.G. Papageorgiou, Optimization-based framework for resin selection strategies in biopharmaceutical purification process development, Biotechnol. Prog. 33 (2017) 1116–1126.
[28] R. Bhambure, A. Rathore, Chromatography process development in the Quality by Design paradigm I: establishing a high-throughput process development platform as a tool for estimating characterisation space for an ion exchange chromatography step, Biotechnol. Prog. 29 (2013) 403–414.
[29] S.H. Ngiam, Y.H. Zhou, M.K. Turner, N.J. Titchener-Hooker, Graphical method for the calculation of chromatographic performance in representing the trade-off between purity and recovery, J. Chromatogr. A 937 (2001) 1–11.
[30] S.H. Ngiam, D.G. Bracewell, Y. Zhou, N.J. Titchener-Hooker, Quantifying process tradeoffs in the operation of chromatographic sequences, Biotechnol. Prog. 19 (2003) 1315–1322.
[31] R.S. Salisbury, D.G. Bracewell, N.J. Titchener-Hooker, A methodology for the graphical determination of operating conditions of chromatographic sequences incorporating the trade-offs between purity and yield, J. Chem. Technol. Biotechnol. 81 (2006) 1803–1813.
[32] S.L.C. Ferreira, R.E. Bruns, E.G. Paranhos da Silva, W.N.L.d. Santos, C.M. Quintella, J.M. David, J.B. de Andrade, M.C. Breitkreitz, I.C.S.F. Jardim, B.B. Neto, Statistical designs and response surface techniques for the optimization of chromatographic systems, J. Chromatogr. A 1158 (2007) 2–14.
[33] D.B. Hibbert, Experimental design in chromatography: a tutorial review, J. Chromatogr. B 910 (2012) 2–13.
[34] V. Kumar, A. Bhalla, A.S. Rathore, Design of experiments applications in bioprocessing: concepts and approach, Biotechnol. Prog. 30 (2013) 86–99.
[35] B. Jones, C.J. Nachtsheim, A class of three-level designs for definitive screening in the presence of second-order effects, J. Qual. Technol. 43 (2011) 1–15.
[36] M. Tai, A. Ly, I. Leung, G. Nayar, Efficient high-throughput biological process characterization: definitive screening design with the Ambr250 bioreactor system, Biotechnol. Prog. 31 (2015) 1388–1395.
[37] G. Carta, A. Jungbauer, Protein Chromatography: Process Development and Scale-Up, WILEY-VCH Verlag CmbH & Co. KGaA, Weinheim, 2010.
[38] S.M. Ross, Introduction to Probability and Statistics for Engineers and Scientists, 4th ed., Elsevier Inc., London, 2009.

Please cite this article in press as: C. Stamatis, et al., High throughput process development workflow with advanced decision-support for antibody purification, J. Chromatogr. A (2019), https://doi.org/10.1016/j.chroma.2019.03.005